Journal of Applied Polymer Science

Preparation of fine fiberglass-resin powders from waste printed circuit boards by different milling methods for reinforcing polypropylene composites

Shuangqiao Yang, Shibing Bai, Qi Wang
State Key Laboratory of Polymer Materials Engineering, Polymer Research Institute of Sichuan University, Chengdu 610065, China
Correspondence to: S. Bai (E-mail: baishibing@scu.edu.cn)

ABSTRACT: In this study, different milling methods were used to prepare fine fiberglass-resin powders (FRP) from waste printed circuit boards for the sake of obtaining high-performance polypropylene (PP)/FRP composite. The processability and appearance of composites can be greatly improved through further milling of FRP; smaller average particle size and narrower particle size distribution can be obtained by pan milling as compared with jet milling and planetary ball milling. Mechanical test results showed that fine FRP prepared by pan milling could be used as reinforcing fillers in the PP composites and possessed better mechanical properties than other two milling methods. The mechanical properties was also confirmed by scanning electron microscopy studies which indicated that the dispersion of FRP and interfacial adhesion between fiberglass and PP matrix was much better by pan milling. Meanwhile, the heterogeneous nucleation effect of FRP by pan milling was more obvious. The above results indicate that solid-state shear is a new method for producing fine FRP and high-performance PP composites filled with FRP. © 2015 Wiley Periodicals, Inc. J. Appl. Polym. Sci. **2015**, *132*, 42494.

KEYWORDS: composites; mechanical properties; recycling

Received 3 March 2015; accepted 12 May 2015
DOI: 10.1002/app.42494

INTRODUCTION

Printed circuit boards (PCBs) is the fundamental component for almost all electronic products and the recycling of waste printed circuit boards (WPCB) is an important subject due to the increase of waste electronic products, not only for the treatment of waste but also for the recovery of valuable materials. The technologies for recycling metals in WPCB progressed greatly and have been widely applied in the last few years[1]; however, it should be noted that the proportion of nonmetals in WPCB reaching nearly 70% is especially difficult for recycling. Millions of tons of nonmetals are generated in the world each year; consequently, how to avoid environmental pollution has become a worldwide problem[2–5] and it is of great importance to develop new methods for recycling nonmetals in WPCB.

Nonmetals in WPCB mainly consist of fiberglass and epoxy resins which cannot be remelted or reformed because of the cross-linked structure of epoxy resins. Thus, the nonmetal materials are landfilled or incinerated directly in most cases, which will cause secondary pollution and result in waste of resources.[6,7] For recycling nonmetal components from WPCB, physical–mechanical technology is drawn mountainous attention and is one of the most effective methods to be used for recycling nonmetals from WPCB. Via this approach, nonmetals in WPCB are usually pulverized into fiberglass-resin powders (FRP) and can be further used as fillers for many products, such as molding electronic components, phenolic molding compound,[8] wood plastic composite,[9,10] modifying nonmetallic plate,[11] and polypropylene (PP) composites.[12–14] However, in the preparation of FRP-reinforced PP composites, some challenges cannot be avoided via conventional preparation methods.[15] On one hand, the processability of PP/FRP composites is poor owing to the relatively higher melting viscosity when compared to pure PP. On the other hand, it is difficult to use PP/FRP composites in practical ways with the poor mechanical properties and the bad appearance. These problems can be attributed to the large FRP particle size and its ununiformed size distribution in the PP matrix. Therefore, new processing technology is necessary in producing fine FRP and high-performance PP/FRP composites. In traditional way researchers sieving fine powders from raw FRP to obtain fine FRP; however, few studies have been found about further pulverizing raw FRP to obtain fine FRP and evaluating pulverizing effect in different milling methods.

The pan-mill is a novel pulverizing instrument which was designed by our laboratory on the basis of the traditional Chinese stone-mill.[16] Due to its unique structure, the pan-mill

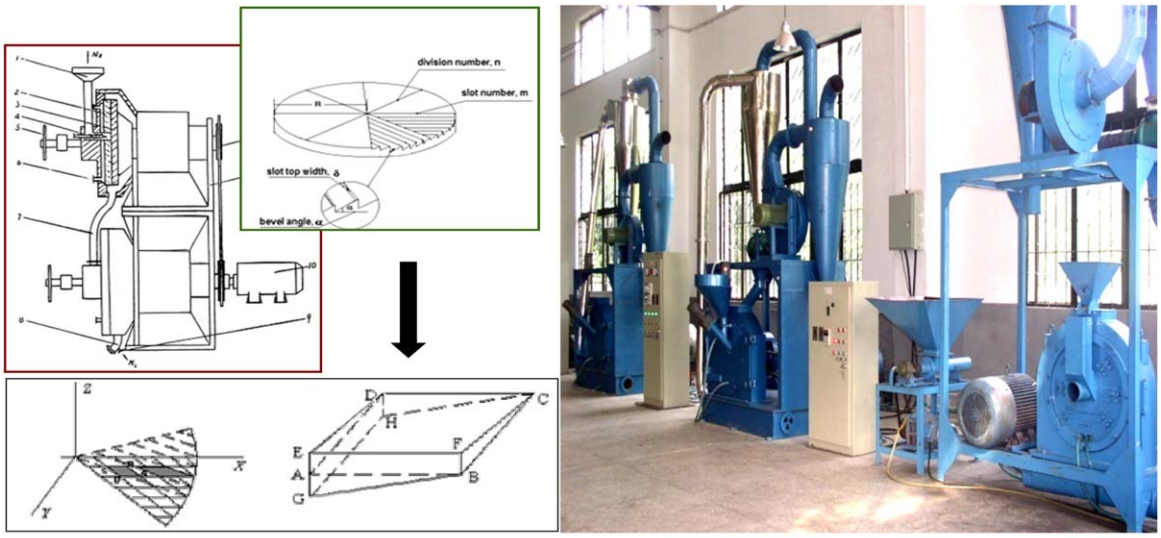

Figure 1. Schematic diagram of (a) pan-mill reactor and (b) pan-mill equipment. [Color figure can be viewed in the online issue, which is available at wileyonlinelibrary.com.]

equipment acted as pairs of three-dimensional scissors during milling, exerting very strong shear force on the milled materials and showing versatile functions such as activation,[17–19] dispersion,[20] mixing,[21] and pulverizing.[22,23] In this study, the fine FRP was prepared by employing traditional pulverization equipment such as ball mill, jet mill, and an environmentally friendly technology—solid-state shear milling (pan milling). The objective of this study is to investigate the pulverizing effect on fine FRP production and the preparation of high-performance PP/FRP composites by jet milling, ball milling, and pan milling. The particle size, particle morphology, crystallization capability, rheological property, mechanical properties, and the appearance of PP/FRP composites were carefully investigated.

EXPERIMENTAL

Materials and Preparation of Fine FRP

In this study, the raw FRP (r-FRP) from WPCB was supplied by a local WPCB factory, which consists of 60–70% fiberglass and 30–40% epoxy resins with an average particle size of 300 μm. The fine FRP was prepared through jet mill (RT-25, Taiwan Hintown Enterprise Co., Ltd., Taiwan, China), ball mill (DECO-PBM-V-2L-B, Changsha Deco Equipment Co., Ltd., Changsha, China), and the self-designed pan-mill equipment (Figure 1) named j-FRP, b-FRP, and p-FRP, respectively. The detailed parameters of the pan-mill equipment can be found in our previous study.[21] The jet milling system can be divided into two parts: grinding system and sorting system. The powder size is guaranteed by adjusting the frequency of the classifier in the sorting system. In this experiment, the classifier frequency was determined as 30 Hz. Furthermore, the grinding gas pressure was set at 0.7 MPa to provide the energy required for crushing powders. Planetary ball milling was performed for 18 h at 120 rpm in a steel jar using steel balls with a diameter of 10 mm and the slurry-to-ball ratio was adjusted to 1 : 1 in volume. The production process of the p-FRP by this self-designed equipment was as follows: the r-FRP was fed to the center of the pan from the inlet, and then driven by shear force, moving along a spiral route toward the edge of the pan until they exited the outlet, which was one cycle of milling process. After the r-FRP was milled for 15 cycles, the p-FRP powders were collected to investigate their morphology and structure, and were used for the preparation of PP/FRP composites.

Preparation of PP/FRP Specimens

The prepared fine FRP were further modified with 2.0 wt % silane-coupling agent KH-550 (Aminopropyltriethoxysilane, Nanjing Shuguang Chemical Group Co. Ltd., China), to improve the compatibility between fine FRP and PP. Before modification, 2 wt % of KH-550 was mixed and hydrolyzed in the solvent (ethanol and water, weight ratio 8 : 2) at 75 rpm in a stirrer for 10 min at room temperature. Subsequently, the modified fine FRP was dried in a vacuum oven at 100°C for 2 h. The modified fine FRP was mixed together with PP (Grade: T30S, Chinese Dushanzi Petrochemical Co., Ltd., China, MFI: 3.6 g/10 min) and polypropylene grafting maleic anhydride (PP-g-MAH, China BlueStar Chenserious Research Institute of Chemical Industry Co. Ltd., China) by a high-speed mixer (WJX-A400, Beijing zhongxingweiye instrument Co., Ltd., China) for 5 min. The mixtures were extruded into thread with a twin-screw extruder (SHJ-20, Nanjing Giant Machinery Co. Ltd., China). The temperature of the extrusion process was 190–210°C and the screw was maintained at a speed of 120 rpm. The test specimens were prepared by a MA1200/370 injection-molding machine (Haitian Plastic Machinery Co., China).

Analytical Methods

Size Analysis. The average particle size and particle size distribution of the fine FRP were measured by a Masterizer 2000 laser particle analyzer (Malvern, Britain).

Morphological Observation. Scanning electron microscope (SEM) (FEI Instrument Co. Ltd, USA) was used to observe the

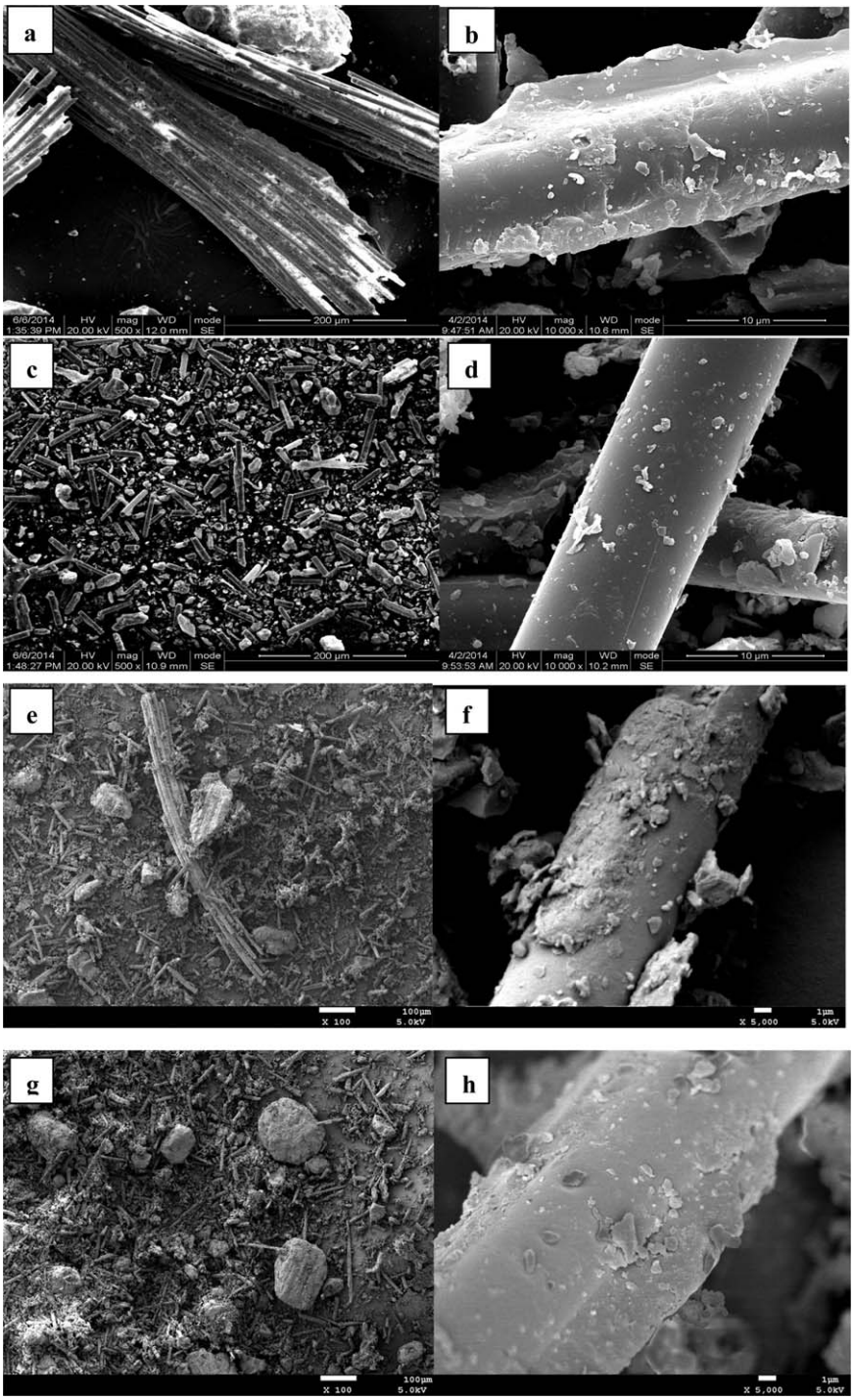

Figure 2. SEM micrograph of (a,b) r-FRP; (c,d) p-FRP; (e,f) b-FRP; (g,h) j-FRP.

morphology of the fine FRP and the brittle fracture face of the injection molded samples. Before SEM evaluation, the samples were sputter-coated with gold to prevent charging during the test.

Mechanical Test. The tensile strength and flexural strength of various samples were tested using a universal testing machine (RG-L-10, Reger Instrument, Co. Ltd, China) at room temperature with a cross-head speed of 50 and 2 mm/min according to ISO 527and ISO 178 standards, respectively. The Charpy impact strength of notched specimens was evaluated according to ISO 179 using a Zwick test instrument (Zwick GbmH & Co. KG, Germany).

Heat Distortion Temperature (HDT) Test. Heat distortion temperature (HDT) values of all kinds of composites were tested on a HDV2 (Atlas Instrument, Co. Ltd, USA) apparatus at a heating rate of 2°C/min and a load of 0.455 MPa according to ASTM D648.

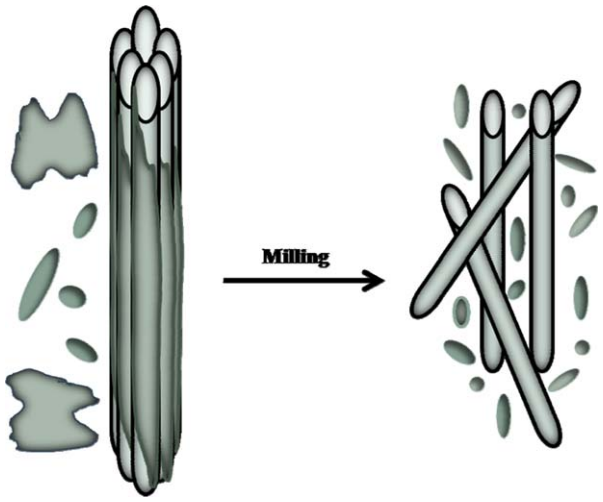

Figure 3. Schematic illustration of effects of pan milling on FRP. [Color figure can be viewed in the online issue, which is available at wileyonlinelibrary.com.]

Differential Scanning Calorimeter (DSC) Analysis. The melting and crystallization behavior of prepared samples were studied using a TA Q20 thermal analyzer (TA Instrument, Co. Ltd, USA). The samples were held at 200°C for 2 min to remove the thermal history. Then, the crystallization and melting curves were obtained by cooling the samples from 200 to 40°C at a rate of 10°C/min, and heating the samples back to 200°C at 10°C/min, respectively. The crystallinity was calculated by the following equation:[24]

$$X_c = \frac{\Delta H_m}{(1-\varphi)\Delta H_c^0} \times 100\%$$

where ΔH_m is the melting enthalpy of samples, ΔH_c^0 is the theoretical value of the melting enthalpy for a 100% crystalline PP which is 209 J/g, and φ is the weight fraction of FRP in the sample.

The Capillary Rheology Test. The capillary rheology measurements were carried out on high-pressure capillary rheometer (Rosand RH7D, Malvern Instruments Co. Ltd, Britain). The sample was first fed in the barrel of the rheometer and preheated for 3 min at 195°C. Subsequently, the measurement was performed in the shear rate range of 100–5000 s^{-1} for all samples.

RESULTS AND DISCUSSION

Characterization of the Fine FRP Prepared by Different Milling Methods

Morphology Observation. In order to investigate the detailed morphological changes of raw FRP (r-FRP) after different milling process, SEM images of the fine FRP under limitation particle size prepared by pan milling (p-FRP), ball milling (b-FRP), and jet milling (j-FRP) are carefully examined, as can be seen in Figure 2. Microscopic observation reveals that r-FRP contains predominantly fiber bundles consisted of glass fiber and epoxy resin shell. Because of hard adhesion between resin and fibers, there are many remaining resins coating on the surface of fiberglass in the r-FRP, resulting in aggregation of fiberglass via the bonding action of resins as shown in Figure 2(a). Figure 2(b) is the high-resolution SEM picture of single fiberglass in r-FRP, with the majority surface of fibers being encapsulated in epoxy resin just like a shell. As shown in Figure 2(c,d), the p-FRP are mainly in the form of single fiberglass and epoxy resin powders, and there is little resin on the surface of fiberglass in p-FRP due to the strong three-dimensional shear forces of pan-mill equipment. The exfoliation effect of epoxy resins from glass fibers can be explained in schematic illustration (Figure 3). The smooth surface of fiberglass is conductive to surface modification, which improves the compatibility between the fiberglass of nonmetals and matrix in composite. Apart from the smooth surface of fiberglass, it is worth noting that no epoxy resin larger than 100 μm can be observed in p-FRP which will lead to less stress concentration when acting as fillers in PP composite. This can result in a consequently higher mechanical property and better processability of composite. In Figure 2(e), it can be seen that b-FRP are mainly in the form of single glass fiber and epoxy resin powders. Fiber bundles also can be observed after planetary ball milling, in which the fiberglass combined together through the bonding action of epoxy resin. Moreover, epoxy resin particles larger than 100 μm can be observed which is inevitable in planetary ball milling due to the pulverization mechanism and this is in accordance with the results of particle size analysis. Because of hard adhesion between resin and fibers, there are many residue resins coating on the surface of fiberglass in b-FRP as illustrated in Figure 2(f) and this is not conductive to surface modification of fiberglass. The morphology of j-FRP is similar to that of b-FRP as shown in Figure 2(g). The j-FRP mainly consisted of single fiberglass and epoxy resin powder, but fiber bundles are not seen. It is clear that there are many epoxy resin particles larger than 100 μm, indicating that it is not easy for the jet stream to grinding the epoxy particles effectively. Meanwhile, the epoxy resin shell coating on the surface of fiberglass is hard to remove during jet milling as shown in Figure 2(h). Furthermore, energy dispersive spectrometer (EDS) was employed to investigate the surface chemical components of fiberglass. As shown in Table I, element contents of carbon and bromine in p-FRP was lower than other FRP, indicating that the brominated epoxy resin could be exfoliated from the surface of fiberglass effectively.

Particle Size Analysis. In this section, the particle size and particle size distribution of fine FRP prepared by different milling

Table I. Elemental Composition on the Surface of Fiberglass by Different Milling Method

	wt %			
Element	r-FRP	p-FRP	b-FRP	j-FRP
C	50.37	15.31	44.70	38.12
O	26.13	42.70	28.05	37.45
Al	2.66	9.35	5.42	1.34
Si	7.37	16.82	5.57	10.45
Ca	6.36	15.27	10.28	8.31
Br	7.12	1.54	6.38	4.32

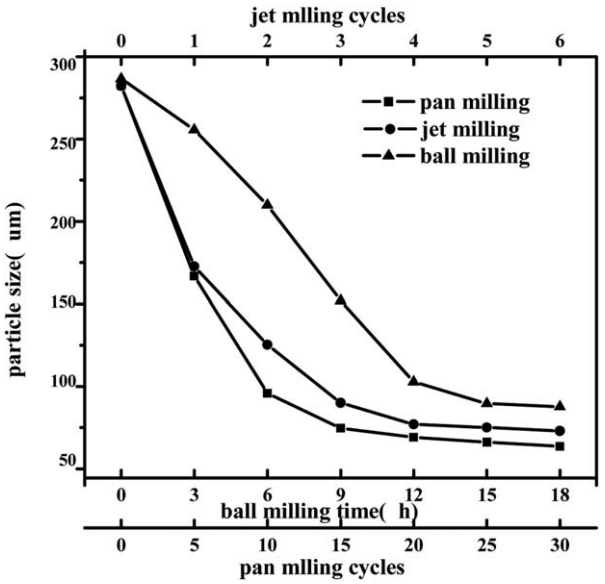

Figure 4. Particle size change of FRP by different milling method.

methods are compared in detail. In Figure 4, the average particle size change of r-FRP after pan milling, jet milling, and ball milling are measured. Obviously, different limitation particle size can be noticed that p-FRP own a lower limitation (61 μm), smaller than that of b-FRP (82 μm) and j-FRP (78 μm). The effect of different milling methods on the differential and cumulative particle size distribution of fine FRP is shown in Figures 5 and 6. The differential distribution curve corresponding to the r-FRP has three distinguished peaks at 650, 85, and 8 μm, corresponding to fiber bundles, single fiberglass, and fine epoxy resin, respectively. After planetary ball milling, the position of peaks in the particle size distribution curve changed little, whereas for jet milling and pan milling, the position of the three peaks shift obviously. The reason for this may be that fiber bundles (between 200 and 1500 μm) exist in grinding powders in planetary ball milling and many epoxy resin particles larger than 100 μm cannot be effectively pulverized in jet milling. For pan milling, however, fiber bundles and large epoxy resin particles disappeared as observed in SEM morphology on the former section.

The difference in the pulverizing effects of pan-mill and traditional pulverization equipment such as ball mill, jet mill, etc. is

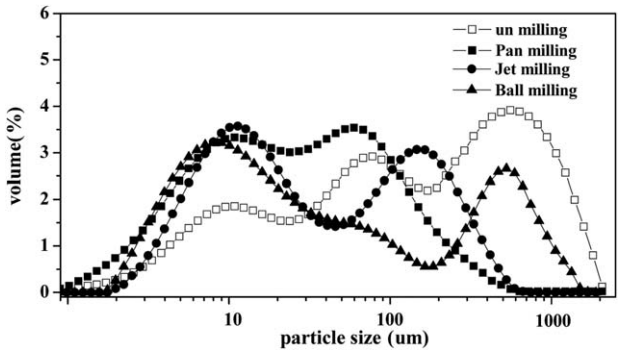

Figure 5. Particle size differential distribution of fine FRP by different milling method.

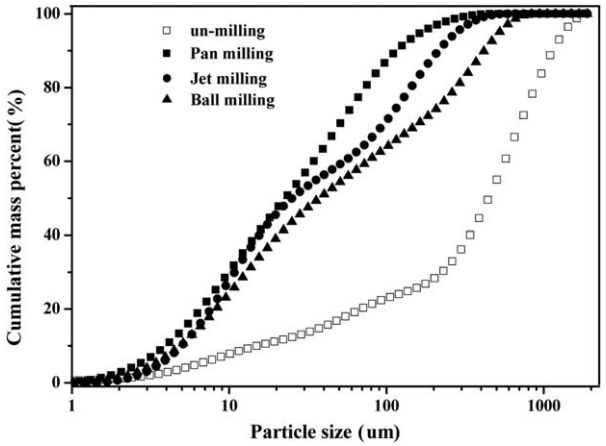

Figure 6. Particle size cumulative distribution of fine FRP by different milling method.

due to their different pulverization mechanisms. Traditional equipments are mainly based on impact force that generates an instantaneous high load. This leads to apparent dissipation of the imported energy, which is disadvantageous to pulverize polymers. However, pan-mill is mainly dependent on three-dimensional shear forces. As the shear forces are imposed on the materials in the whole milling process of the material particles along the spiral route, therefore, the continually increasing elastic deformation can quickly reach the limitation that macromolecular chains can endure and causes the rapid breakage of bulk materials. Based on the above pulverizing mechanism, pan-mill equipment shows outstanding advantage in pulverizing raw-FRP and epoxy resins as demonstrated in this section.

Characterization of PP/FRP Composites Prepared by Different Milling Methods

Morphology Observation. The physical performance of reinforcing material strongly depends on the dispersion of fillers in matrix. In general, better dispersion of fillers and strong interfacial adhesion between matrix and fillers permits better mechanical properties, which can be proved by comparing the liquid-nitrogen-fractured surface SEM micrographs of specimens. Figure 7 shows the SEM micrograph of the fracture surface of composite filled with r-FRP and fine FRP prepared by different milling method. Figure 7(a) shows the SEM micrograph of the fracture surface of composite filled with r-FRP. On the fracture surface of the composite, fiber bundles observed clearly in the matrix and crevices between epoxy resin powder and pp matrix is obvious, which is easy for the crack initiation and particles to detach themselves from the polymer matrix. Figure 7(b) shows the SEM micrograph of the fracture surface of composite filled with p-FRP. As expected, the fillers are dispersed uniformly in the matrix and no fiber bundles and large epoxy resin powder can be seen. The fine particle size lead to less stress concentration in PP matrix and this would be beneficial to improve the mechanical properties of composite. Figure 7(c,d) shows the SEM micrograph of the fracture surface of composite filled with j-FRP and b-FRP, respectively. Dispersion of fine FRP in the PP matrix seems to be good but epoxy resin powder about 100 μm can be observed when composite filled with j-FRP. However, in

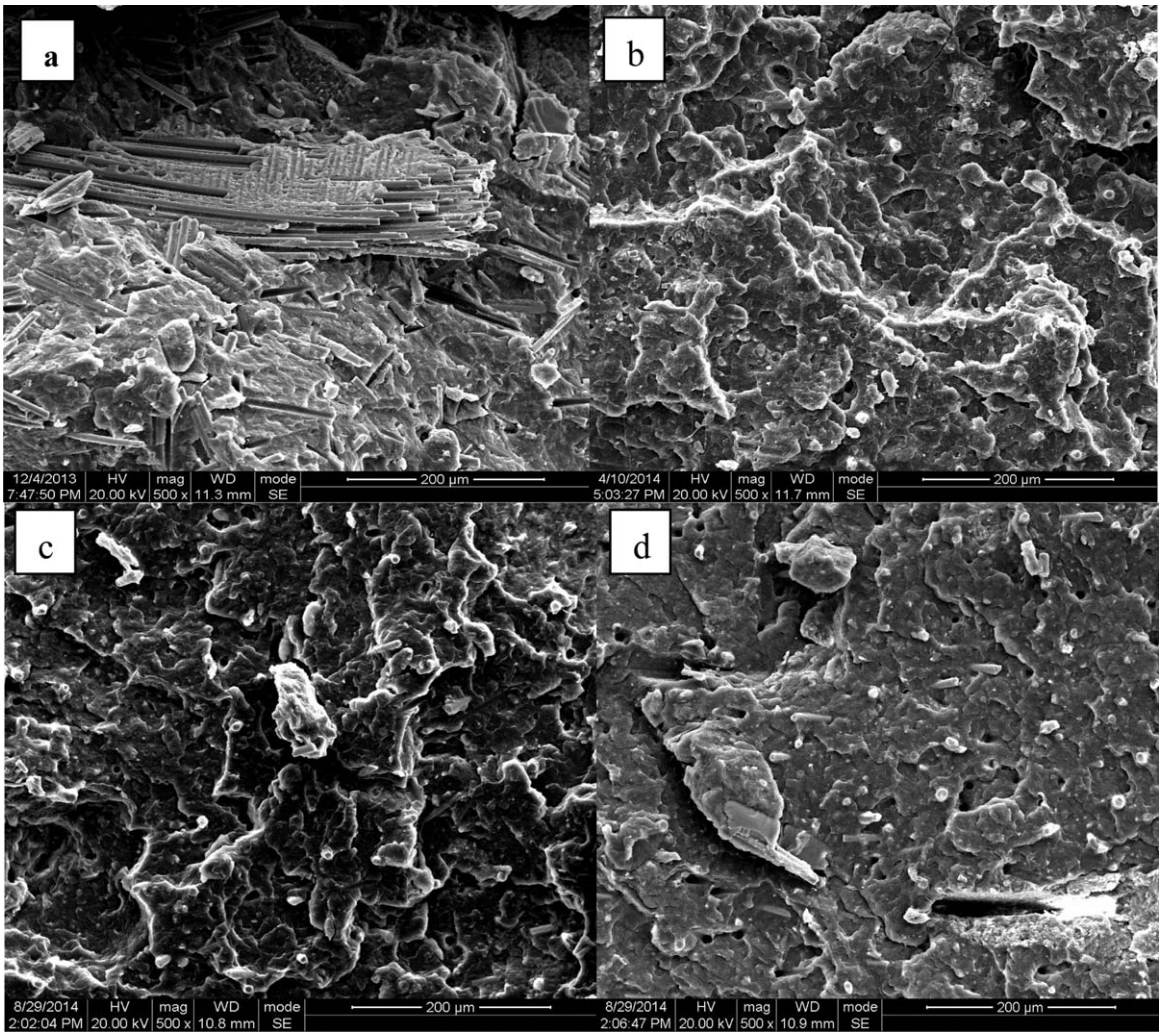

Figure 7. SEM micrograph of composites filled with fine FRP after milling: (a) un-milling, (b) pan milling, (c) jet milling, (d) ball milling.

composite filled with b-FRP, both fiber bundles (the pull-out holes) and large epoxy resin powder can be found, which may give rise to stress concentration and easy for crack propagation.

Crystallization and Melting Properties. The milling and dispersed FRP in PP matrix are expected to influence physical properties of composites, so DSC tests were carried out to investigate the effects of milling on the crystallization behavior of PP. DSC curves of PP/FRP composites are shown in Figure 8, and the corresponding DSC data, such as melting and crystallization temperatures (T_m and T_c), melting enthalpy (ΔH_m), and degree of crystallinity (X_c) were summarized in Table II. It can be seen that the addition of fine FRP has no remarkable effect on the T_m of PP, but the X_c obviously increased. The result suggests that fine FRP did not change crystalline structure of PP but can act as nucleation agents on the polymer matrix during nonisothermal crystallization and the heterogeneous nucleation effect of fine FRP can improve the crystallization capability of PP, thus improve the mechanical properties of composite. The addition of p-FRP improved the X_c of PP from 33 to 43%, greater than j-FRP (36%) and b-FRP (37%) as shown in Table II. This may be attributed to that the increase of specific surface is caused by reduced particle size of r-FRP during pan milling. Obviously, the crystallization temperatures (T_c) of the composites filled with fine FRP are higher than that of pure PP (115.7°C), identifying the nucleation effect of inorganic fillers on the crystallization of PP, also. Furthermore, T_c of composite filled with p-FRP (126.33°C) is higher than that of composites filled with j-FRP (124.29°**C**) and b-FRP (123.86°**C**), showing the stronger nucleation effect of FRP on PP. This result agrees with the values of X_c. Thus we can conclude that the nucleation effect of p-FRP can more greatly improve the crystallization of PP, due to the increase of specific surface caused by a smaller average particle size.

Mechanical Properties. The mechanical properties of PP/FRP composites with different milling methods are shown in Table III. Tensile strength and flexural strength of composite with p-FRP are obviously greater than those prepared by other milling methods; the tensile strength increased from 32.3 to 39.1 MPa, flexural strength increased from 50.6 to 54 Mpa, and flexural modulus increased from 1.7 to 1.9 Gpa, respectively. This is

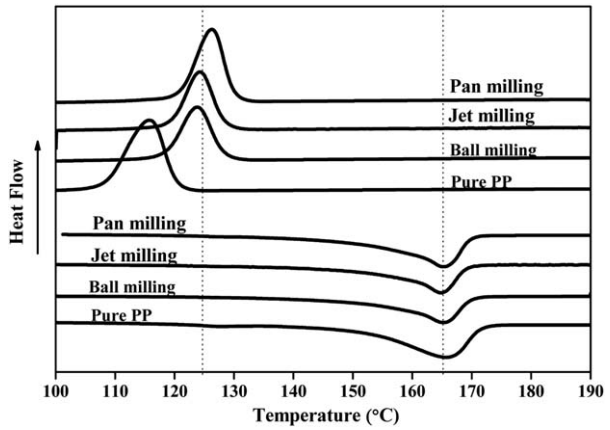

Figure 8. Effect of FRP on melting and crystalline properties of PP/FRP composite (30 wt %).

mainly because b-FRP and j-FRP contains many fiber bundles and large epoxy resin particles which can easily increase the probability of stress concentration, cracks can travel around the stress concentrations and propagate with less energy. However, after pan milling, the particle size of p-FRP is smaller, leading to a greater increase in interfacial contact area and this would be beneficial to transfer the stress from the PP matrix to fillers. In addition, the smooth surface of fiberglass in p-FRP is easy to surface modification and this can improve the compatibility between fiberglass and PP. Nevertheless, in b-FRP and j-FRP, the residue epoxy resins coating in the fiberglass surface directly contact with pp matrix and the weak interfacial adhesion between the epoxy resin and matrix leading to ineffective transfer of the applied stresses through the interface, therefore, resulted in lower tensile strength and flexural strength of the composite. However, for impact strength, there is no obvious difference between composites filled with fine FRP by different milling methods, but all of them are slightly greater than that of the pure PP. In this study, it is clearly shown that p-FRP can be used as reinforcing fillers in polypropylene composites and possessed better mechanical properties than that of b-FRP and j-FRP.

The Rheological Properties. The choice of suitable processing conditions and composite formulations is guided mainly by the rheological behavior of composites, so an investigation of capillary rheological properties of filled molten polymers is of fundamental and practical importance. Figure 9 shows the effect of different milling methods on the melt viscosity of PP/FRP composite. It can be noticed that the viscosity of composite filled with r-FRP increased far more than composite filled with milling fillers at the same shear rate. But the milling methods did not show markedly influence on apparent viscosity of PP/FRP composites at all shear rate in this research. In other words, the processability of PP/FRP composite can be obviously improved through milling, whereas did not show great variation for different milling methods. In r-FRP system, the dispersion of fillers is not so fine and at the same time, the long fiberglass and fiber bundles are difficult to orient in the direction of melt flow. This is associated with more hindrance to the mobility of pp molecular chains with increasing aspect ratio of filler. Generally, fillers will perturb the normal flow of polymer matrix and hinder the mobility of chain segments in flow in filled system. However, fillers having smaller particle size and shorter length are more easily aligned along the direction of flow and less hinder the mobility of polymer chain than longer fillers, which may prove to be highly valuable in practical application.

Table II. DSC Date of PP/FRP Composites (30 wt %)

Sample	T_m (°C)	ΔH_m (J·g^{-1})	T_c (°C)	X_c
Pure PP	165.67	69.63	115.70	0.33
Pan milling	165.24	63.29	126.33	0.43
Jet milling	164.72	52.25	124.29	0.36
Ball milling	165.26	53.89	123.86	0.37

The Appearance of Composites. As an industrial product, the appearance of the recycled PCB products is of great importance as it should be accepted by users in practical application. In this section, the appearances of composites filled with r-FRP, p-FRP, j-FRP, and b-FRP are compared in detail. A lot of macular can be observed on product surface as presented in Figure 10(a), which can seriously affect the mechanical properties of final products. This can be attributed to the big particle size of FRP and uneven distribution of FRP in the pp matrix. The appearance of PP composite filled with fine FRP by three different milling method is improved greatly due to the particle size reduce of FRP and even distribution of FRP in the pp matrix as shown in Figure 10(b–d).

CONCLUSIONS

In summary, this study showed that fine FRP can be successfully prepared via further milling, whereas, some troubles were inevitable in further pulverizing r-FRP during jet milling and ball milling due to their pulverization mechanisms. The results of SEM and particle size analysis show that p-FRP own a lower limitation particle size (61 μm), smaller than the limitation particle size of b-FRP (82 μm) with fiber bundles (between 200 and 1500) and j-FRP (78 μm) with many epoxy resin particles larger than 100 μm, which means the pan-mill equipment had

Table III. Mechanical Properties of PP/FRP (30%) Composites by Different Milling Method

Milling method	Tensile strength (Mpa)	Elongation at break (%)	Flexural strength (Mpa)	Flexural modulus (Gpa)	Impact strength (KJ/m^2)
Pure pp	32.3 ± 0.9	73.3 ± 2.6	50.6 ± 1.9	1.7 ± 0.12	2.6 ± 0.21
Pan milling	39.1 ± 0.6	20.3 ± 2.3	54.4 ± 2.1	1.9 ± 0.04	2.7 ± 0.15
Jet milling	35.2 ± 0.8	22.6 ± 1.8	43.2 ± 1.4	1.3 ± 0.08	2.7 ± 0.24
Ball milling	35.6 ± 0.4	21.8 ± 2.4	42.4 ± 1.7	1.2 ± 0.07	3.0 ± 0.31

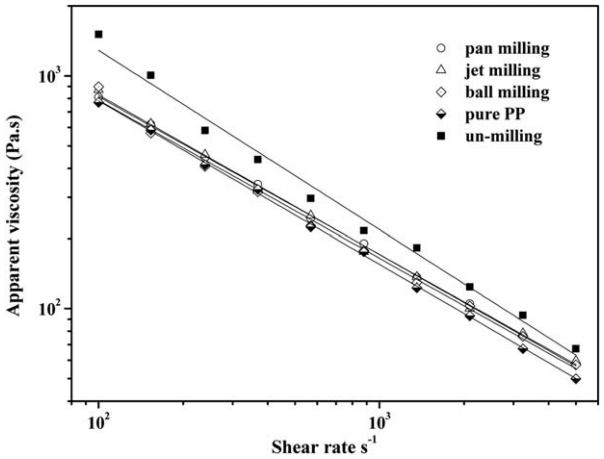

Figure 9. The apparent viscosity of PP/FRP composite (30%).

advantage in further pulverizing r-FRP. Consequently, in SEM micrograph of the fracture surface of composite filled with r-FRP, fillers are dispersed uniformly in the matrix and no fiber bundles and large epoxy resin powder can be seen resulting in a better mechanical properties than that of pure PP and PP composites filled with b-FRP and b-FRP as confirmed by mechanical test. Furthermore, the DSC result indicated that the addition of p-FRP can obtain more pronounced heterogeneous nucleation effect of the resulting PP/FRP composites with the X_c of PP increased from 33 to 43%, greater than j-FRP (36%) and b-FRP (37%), benefiting to improve the mechanical properties of composite. In addition, the processability and appearance of composite significantly improved in all three different milling methods, which can be attributed to the decrease of particle size under milling.

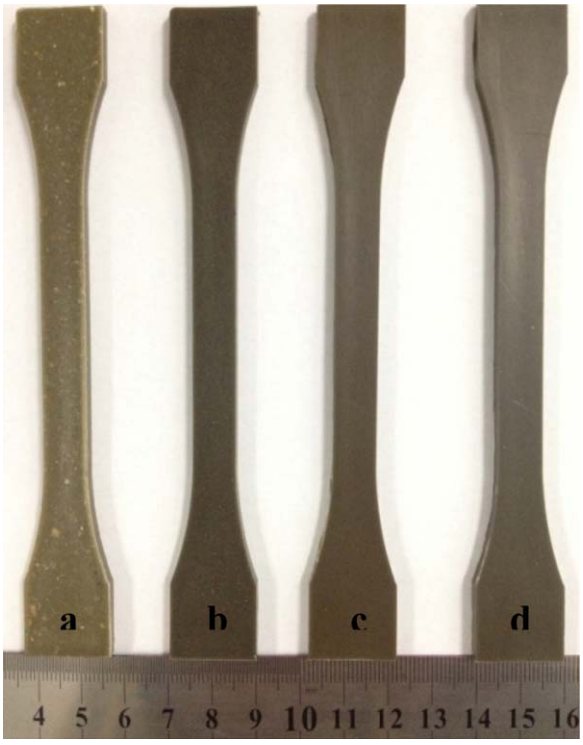

Figure 10. Image of PP/FRP composite (30%): (a) r-FRP; (b) p-FRP; (c) j-FRP; (d) b-FRP. [Color figure can be viewed in the online issue, which is available at wileyonlinelibrary.com.]

It is thus concluded that pan milling can act as a new technology and new method for the high-value recycling of wasted circuit boards and producing PP/FRP composites.

ACKNOWLEDGMENTS

This project was supported by the National High Technology Research and Development Program of China (863 program 2012AA063003).

REFERENCES

1. Veit, H. M.; Bernardes, A. M.; Ferreira, J. Z.; Tenorio, J. A. S.; de Fraga Malfatti, C. *J. Hazard. Mater.* **2006**, *137*, 1704.
2. LaDou, J. *Int. J. Hyg. Environ. Health* **2006**, *209*, 211.
3. Cui, J.; Forssberg, E. *J. Hazard. Mater.* **2003**, *99*, 243.
4. Kalantar, Z. N.; Karim, M. R.; Mahrez, A. *Constr. Build. Mater.* **2012**, *33*, 55.
5. Zhou, L.; Xu, Z. *Environ. Sci. Technol.* **2012**, *46*, 4713.
6. Leung, A.; Cai, Z.; Wong, M. *J. Mater. Cycles Waste Manage.* **2006**, *8*, 21.
7. Leung, A. O.; Luksemburg, W. J.; Wong, A. S.; Wong, M. H. *Environ. Sci. Technol.* **2007**, *41*, 2730.
8. Guo, J.; Rao, Q.; Xu, Z. *J. Hazard. Mater.* **2008**, *153*, 728.
9. Guo, J.; Tang, Y.; Xu, Z. *Environ. Sci. Technol.* **2010**, *44*, 463.
10. Guo, J.; Tang, Y.; Xu, Z. *J. Hazard. Mater.* **2010**, *179*, 203.
11. Guo, J.; Guo, J.; Wang, S.; Xu, Z. *Environ. Sci. Technol.* **2009**, *43*, 503.
12. Zheng, Y.; Shen, Z.; Cai, C.; Ma, S.; Xing, Y. *J. Hazard. Mater.* **2009**, *163*, 600.
13. Zheng, Y.; Shen, Z.; Cai, C.; Ma, S.; Xing, Y. *Mater. Des.* **2009**, *30*, 958.
14. Åkesson1, D.; Krishnamoorthi, R.; Foltynowicz, Z.; Christéen, J.; Kalantar, A.; Skrifvars, M. *Polym. Polym. Compos.* **2013**, *21*, 333.
15. Hong, S. G.; Su, S. H. *J. Environ. Sci. Heal.* **1996**, *31*, 1345.
16. Wang, Q.; Cao, J.; Huang, J.; Xu, X. *Polym. Eng. Sci.* **1993**, *37*, 1091.
17. Zhang, W.; Liang, M.; Lu, C. *Cellulose* **2007**, *14*, 447.
18. Zhang, X.; Lu, Z.; Tian, D.; Li, H.; Lu, C. *J. Appl. Polym. Sci.* **2013**, *127*, 4006.
19. He, X.; Zhang, X.; Zhang, W.; Tian, D.; Lu, C. *J. Vinyl Addit. Tech.* **2014**, *20*, 177.
20. Albert, D.; Naomi, F.; Andrew, H. L. Solid-state shear pulverization: A novel process for efficient mixing and compatibilization of polymer blends. Proceedings of Third Joint China/USA Chemical Engineering Conference, Beijing, **2000**.
21. Zhang, X.; Lu, C.; Liang, M. *J. Appl. Polym. Sci.* **2007**, *103*, 4087.
22. Chen, Z.; Liu, C.; Wang, Q. *Polym. Eng. Sci.* **2001**, *41*, 1187.
23. Xu, X.; Wang, Q.; Kong, X. A.; Zhang, X. D.; Huang, J. G. *Plast. Rubber Compos.* **1996**, *25*, 152.
24. Jiang, X.; Drzal, L. T. *Polym. Compos.* **2012**, *33*, 636.